Beam acceleration by plasma-loaded free-electron devices

K. H. Tsui, A. Serbeto, and J. B. D'Olival
Instituto de Fisica, Universidade Federal Fluminense, Gragoata, 24210-340 Niteroi, Rio de Janeiro, Brazil
(Received 8 October 1996; revised manuscript received 31 March 1997)

The use of a plasma-filled wiggler free-electron laser device operating near the plasma cutoff to accelerate electron beams is examined. Near the cutoff, the group velocity of the microwave field in the plasma is much less than the beam velocity. This scheme, therefore, operates in the pulse mode to accelerate electron beam bunches much shorter than the wiggler length. Between one bunch and the other, the wiggler is reloaded with microwave field. During the loading period, the laser-wiggler-plasma (SWL) Raman interaction generates a Langmuir mode with the laser and the wiggler as the primary energy sources. When the wiggler plasma is fully loaded with microwave field, a short electron bunch is fired into the device. In this accelerating period, the Langmuir mode is coupled to the laser-wiggler-beam (SWB) free-electron-laser interaction. The condition that the Langmuir phase velocity matches the free-electron-laser resonant beam velocity assures the simultaneous interaction of the SWL and SWB parametric processes. Beam acceleration is accomplished fundamentally via the space charge field of the Langmuir mode and the electron phase in the ponderomotive potential. Linear energy gain regime is accomplished when the phase velocity of the Langmuir mode is exactly equal to the speed of light. [S1063-651X(98)06701-4]

PACS number(s): 52.75.Di, 52.75.Ms, 52.35.Nx

I. INTRODUCTION

Free-electron devices such as the cyclotron autoresonance maser and the free-electron laser are powerful devices to generate intense electromagnetic radiations in laboratories and also in solar coronas [1]. These systems are based on the parametric interaction among the electron beam, the wiggler, and the radiation field. The inverse application of these devices can accelerate electron beams by using the radiation field as the primary energy source. The attainable beam energy depends on the power and energy of the radiation field. To work at the optical frequency with powerful lasers requires very small wiggler periods due to the free-electron-laser parameter scaling. To accelerate electrons to the 100 GeV range calls for kilometric size wigglers [2]. Other rivaling mechanisms such as beat wave, wake field, and surfatron use a background plasma medium to achieve high gradient accelerations [3–6]. In these schemes, intense lasers are used to generate a Langmuir wave in the background plasma through the ponderomotive force of either a single short pulse for wake field or a train of such pulses for beat wave configurations. The lasers are operating high above the plasma cutoff while keeping the beat frequency near the plasma frequency. The electron beam then interacts directly with the space charge field. Recent experiments have proved the working principles of the beat wave acceleration with great sucess [7,8].

In a classical free space free-electron laser configuration, the static magnetic field wiggler is equivalent to a head-on electromagnetic wave in the beam frame of the electrons. This plus the forward propagating wave in a plasma loaded wiggler form an equivalent beat wave system to the laboratory frame laser beat wave unit. Here, we consider this plasma-loaded wiggler free-electron acceleration device [9–12]. In Ref. [9], Bobin has considered the two stream beam-plasma mode whose frequency is much higher than the plasma frequency. Parametric coupling among the laser field, the strong wiggler, and the beam-plasma mode then leads to beam acceleration or laser emission through the space charge field. The analysis is only qualitative, and is limited to order of magnitude estimates. In this scenario, the device works in a continuous state sustained by the space charge field of a long beam. In Ref. [12], Maroli *et al.* have suggested operating the plasma-loaded device near the cutoff using very strong wiggler fields. Their calculation has assumed that the background gets relativistic because of the static wiggler field [13]. This evidently violates energy conservation of the background plasma [14]. Their background plasma has a transverse velocity due to the static wiggler field. This velocity would contribute to a relativistic transverse current for a huge wiggler field in the wave equation of the laser field. We believe this wiggler-dependent transverse velocity of the background plasma is incorrect. Furthermore, neither of the two publications treats the relative phases of the laser field and Langmuir mode. The evolutions of these relative phases are as important as their corresponding field amplitudes in determining the parameters of an accelerator design.

Here, we reconsider the plasma-loaded wiggler in the same spirit of Bobin but taking into consideration the relative phases and frequency mismatches. However, we aim to operate the device near the cutoff with some essential differences with earlier publications. First, we remark that the group velocity of the laser field is very small in this situation so that the device has to be operated in short beam pulses. Between one beam pulse and the other, the wiggler plasma is reloaded with laser field throughout. Second, the Langmuir mode is driven by the ponderomotive force of the laser and wiggler fields, and not by single pulse or pulse train. Third, the electron beam then interacts simultaneously with both the Langmuir space charge field through the Raman interaction, and the wiggler and laser fields through the free-electron laser resonance interaction. The electron beam is then accelerated efficiently through the space charge field and the relative phase of the ponderomotive potential. This is the prime

motive for loading the wiggler with plasma. Fourth, the operating frequency (millimeter) of this configuration is much lower than the two-laser (optical) beat wave configuration.

II. LANGMUIR MODE EXCITATION

The interaction of a low density electron beam (B) with a laser field (S) under a magnetic wiggler (W) filled with a low temperature high density plasma (L) can be divided into two parametric interactions. The first is the laser-wiggler-plasma (SWL) Raman interaction, which excites the Langmuir wave. The second is the laser-wiggler-beam (SWB) free electron laser resonant interaction. Matching the operating conditions of these two processes, the Langmuir wave can accelerate the electron beam through the space charge field.

Operating near the cutoff frequency, the group velocity in the wiggler plasma is very slow. Therefore, it is necessary to load the wiggler plasma first with microwave field. During this phase, only the SWL Raman interaction takes place, and the Langmuir mode can be generated through the microwave and the wiggler. From basic SWL derivations, the background plasma with density N satisfies the following equation, which describes the density perturbation δN:

$$\left\{\frac{\partial^2}{\partial t^2}-v_e^2\frac{\partial^2}{\partial z^2}+\frac{1}{\gamma}\omega_p^2\right\}\frac{\delta N}{N}=\frac{c^2}{4\gamma^2}\frac{\partial^2}{\partial z^2}\left(\frac{q\vec{A}}{mc^2}\cdot\frac{q\vec{A}}{mc^2}\right), \tag{1}$$

where γ is the Lorentz factor for the background plasma, and $\vec{A}=\vec{A}_w+\vec{A}_s$ is the total vector potential of the wiggler and laser fields. Furthermore, the vector potential of the laser field and the scalar potential Φ of the space charge field are described by

$$\left\{\frac{\partial^2}{\partial t^2}-c^2\frac{\partial^2}{\partial z^2}+\frac{1}{\gamma}\omega_p^2\right\}\frac{q\vec{A}_s}{mc^2}=-\frac{\omega_p^2}{\gamma}\frac{\delta N}{N}\frac{q\vec{A}_s}{mc^2}, \tag{2}$$

$$\frac{\partial^2}{\partial z^2}\frac{q\Phi}{mc^2}=-\frac{\omega_p^2}{c^2}\frac{\delta N}{N}. \tag{3}$$

We observe that Eq. (2) is different from the usual beat wave scheme with two laser fields where both fields drive a transverse velocity in the background plasma. In our case, the static wiggler field does not drive such a velocity. This eliminates the δNA_w parametric term in Eq. (2) and leaves only the δNA_s term. For the same reason, the parametric term in Eq. (1) is only half of what it is in standard beat wave derivations. We consider the following harmonic dependences in (z,t) with slowly varying amplitudes and relative phases: $\vec{A}_s=A_{s0}\sin(k_sz-\omega_st+\phi_s)\vec{y}$, $\vec{A}_w=A_{w0}\sin(k_wz)\vec{y}$, $\delta N=\delta N_0\sin(k_Lz-\omega_Lt+\phi_L)$, and $\Phi=\Phi_0\sin(k_Lz-\omega_Lt+\phi_L)$. The laser and Langmuir modes are governed by their respective dispersion relations,

$$\omega_s^2=\frac{1}{\gamma}\omega_p^2+c^2k_s^2, \tag{4}$$

$$\omega_L^2=\frac{1}{\gamma}\omega_p^2+v_e^2k_L^2. \tag{5}$$

Since the magnetic wiggler is static, the Raman interaction requires $\omega_s=\omega_L$, therefore, the laser mode is operating near the plasma cutoff, and k_s is nearly zero. If the plasma loaded wiggler length is less than $2\pi/k_s$, the laser field has a spatially uniform but time varying amplitude A_{s0} inside the plasma. Since this is the primary free energy source, the driven Langmuir mode has also a time varying only amplitude δN_0 with $k_L\gg k_s$. With the above considerations in mind, and using the eikonal approximations, which requires $\partial A_{s0}/\partial t\ll\omega_sA_{s0}$, $\partial A_{s0}/\partial z\ll k_sA_{s0}$, and likewise for other field variables, the Raman interaction with

$$\psi_L=\psi_s+\psi_w, \tag{6}$$

where $\psi_w=k_wz$, $\psi_s=k_sz-\omega_st$, and $\psi_L=k_Lz-\omega_Lt$ are the harmonic phases, is described by

$$2\omega_L\left[\frac{da_p}{dt}\right]\cos(\psi_L+\phi_L)-2\omega_La_p\left[\frac{d\phi_L}{dt}\right]\sin(\psi_L+\phi_L)=-\frac{c^2k_L^2}{4\gamma^2}a_sa_w\cos(\Delta\phi)\cos(\psi_L+\phi_L)$$
$$-\left[\frac{c^2k_L^2}{4\gamma^2}a_sa_w\sin(\Delta\phi)-(\Delta\omega_L^2)a_p\right]\sin(\psi_L+\phi_L), \tag{7}$$

$$2\omega_s\left[\frac{da_s}{dt}\right]\cos(\psi_s+\phi_s)-2\omega_sa_s\left[\frac{d\phi_s}{dt}\right]\sin(\psi_s+\phi_s)=\left[\frac{1}{\gamma}\omega_p^2a_p\sin(\psi_L+\phi_L)+(\Delta\omega_s^2)\right]a_s\sin(\psi_s+\phi_s), \tag{8}$$

$$\phi=\frac{\omega_p^2}{c^2k_L^2}a_p, \tag{9}$$

where $a_w = qA_{w0}/mc^2$, $a_s = qA_{s0}/mc^2$, $a_p = \delta N/N$, $\phi = q\Phi/mc^2$, and $\Delta\phi = \phi_L - \phi_s$. Also, $\Delta\omega_s^2 = \omega_p^2/\gamma + c^2k_s^2 - \omega_s^2$, and $\Delta\omega_L^2 = \omega_p^2/\gamma + v_e^2k_L^2 - \omega_L^2$ are the frequency mismatches. The total derivatives in Eqs. (7) and (8) are characterized by the Langmuir and laser group velocities respectively in the convective part. If the dispersion relations are exactly satisfied, there will be no mismatches. For a small plasma density deviation, the mismatches are nonzero. Since the density appears equally in both Eqs. (4) and (5), and also since $\omega_s = \omega_L$, the two mismatches are always the same with $\Delta\omega_s^2 = \Delta\omega_L^2$. For electron temperature deviations, which appear in Eq. (5) only, the two mismatches will be different.

III. BEAM ACCELERATION

When the plasma-filled wiggler is fully loaded with microwave field, and the Langmuir mode is generated, a short electron bunch is fired into the device. During this brief moment when the beam traverses the wiggler, both *SWL* and *SWB* interactions take place simultaneously. Since the transit time of the beam is almost negligible compared to the loading time of the wiggler plasma, and also since the beam density is usually much lower than the background plasma, the feedback of the beam on the Langmuir mode of Eq. (7), in the presence of the large parametric driving force, is not considered. The beam inteacts with the system through the free-electron-laser *SWB* resonance; which relies on the resonant condition

$$\omega_s - k_s v_z = k_w v_z, \tag{10}$$

stating that the Doppler shifted laser frequency is equal to the wiggler frequency in the beam frame. The energy and phase of each beam electron in the ponderomotive potential are given by

$$\left[\frac{d\gamma_j^2}{dt}\right] = -\omega_s a_s a_w \cos(\Delta\phi)\sin(\psi_j + \phi_L) + \left[\omega_s a_s a_w \sin(\Delta\phi) - \frac{2\gamma_j\beta_j\omega_p^2}{ck_L}a_p\right]\cos(\psi_j + \phi_L), \tag{11}$$

$$\left[\frac{d\psi_j}{dt}\right] = ck_L(\beta_{z_j} - \beta_L), \tag{12}$$

respectively, where we have used Eq. (9) to obtain the a_p term in Eq. (11), and $\beta_z = v_z/c$ and $\beta_L = \omega_L/ck_L$. The convective part of this total derivative carries the beam velocity v_z.

The action of the Langmuir mode is exercised through the a_p term and the relative phase ϕ_L in Eq. (11). The Langmuir wave has a phase velocity ω_L/k_L, which can trap the beam electrons with equal velocity $v_z = \omega_L/k_L$. Although the Raman scattering can operate on $\psi_L = \psi_s \pm \psi_w$ modes, we have particularly chosen the upper sign. The fundamental reason is that, with $\psi_L = \psi_s + \psi_w$, the beam velocity satisfies

$$v_z = \frac{w_L}{k_L} = \frac{w_s}{k_s + k_w}, \tag{13}$$

which is compatible with Eq. (10) for the free-electron-laser resonant condition. This coupling allows the simultaneous *SWL* and *SWB* interactions.

IV. ALONG THE CHARACTERISTICS

The first order partial differential equation that we are considering can be transformed into a set of ordinary differential equations along the characteristic [15,16]. Following this representation, we write the equations along the laser, and beam characteristics with $z_s = v_{gs}t$, and $z_b = v_z t$. Physically, this means following the evolution of the relevant field in its own frame of energy transmission. For the laser field, we are following the same wave packet. For the beam, we are following a fixed ensemble of beam electrons interacting with the spatially uniform fields. The electron phase in the ponderomotive well is $\psi_j = k_L z_{bj}(t) - \omega_L t$. Since the Langmuir group velocity is much smaller than the laser group velocity, which is already small in the plasma, we take $v_{gL} = 0$. The partial time derivative of the Langmuir mode in Eq. (7) can be expressed in terms of the laser characteristic. The equations now read

$$2\omega_L v_{gs}\frac{da_p}{dz_s} = -\frac{(ck_L)^2}{4\gamma^2}a_s a_w \cos\Delta\phi, \tag{14}$$

$$2\omega_L v_{gs}\frac{d\phi_L}{dz_s} = \frac{(ck_L)^2}{4\gamma^2}\frac{a_s a_w}{a_p}\sin\Delta\phi - (\Delta\omega_L^2), \tag{15}$$

$$2\omega_s v_{gs}\frac{da_s}{dz_s} = 0, \tag{16}$$

$$2\omega_s v_{gs}\frac{d\phi_s}{dz_s} = -\frac{\omega_p^2}{\gamma}a_p \sin(\psi_L + \phi_L) - (\Delta\omega_s^2), \tag{17}$$

$$v_z\frac{d\gamma_j^2}{dz_b} = -\omega_s a_s a_w \cos\Delta\phi \sin(\psi_j + \phi_L) + \left[\omega_s a_s a_w \sin\Delta\phi - \frac{2\gamma_j\beta_j\omega_p^2}{ck_L}a_p\right]\cos(\psi_j + \phi_L), \tag{18}$$

$$v_z\frac{d\psi_j}{dz_b} = ck_L(\beta_{z_j} - \beta_L), \tag{19}$$

where we have equated the sine and cosine terms independently. The Langmuir mode a_p in Eq. (14) is linear in z_s when $\Delta\phi$ is small. It saturates when the cosine factor begins to take action. The saturation level depends more on the rate where $\Delta\phi$ becomes significant than on the product $a_s a_w$, which determines the initial linear growth rate. The evolution of $\Delta\phi$ along the wiggler is given by Eqs. (15) and (17). From Eq. (16), the laser field amplitude a_s is constant. This result is based on linear perturbation analysis, which requires $a_p \ll 1$. Should a_p be large, the dispersion relation of a_s, according to Eq. (2) including δN, would lead to a cutoff frequency with large fluctuation where the propagation of the laser field is prejudiced. The acceleration of an electron bunch in the established Langmuir mode is described by Eqs. (18) and (19). For the parameters that we are considering below, the dominant term in Eq. (18) is the Langmuir mode.

V. OPERATING PARAMETERS

From the dispersion relations given by Eqs. (4) and (5), with $\omega_s=\omega_L$, we have $k_s=(v_e/c)k_L=\mu k_L$ and from $k_L=k_w+k_s$ we have $k_L=k_w/(1-\mu)$. The wave vectors are, therefore, specified by the wiggler period. For a given plasma density N, the mode frequency is then given by the plasma dispersion relation $\omega_L^2=\omega_s^2=\omega_p^2/\gamma+(\mu c k_L)^2$. The Langmuir phase velocity ω_L/k_L can thus be chosen in terms of ω_p, μ, and k_w. We consider plasma temperature $T_e=1$ eV, density $N=1.2\times10^{13}/\mathrm{cm}^3$, initial energy $\gamma(0)=1$, wiggler period $\lambda_w=1$ cm, initial beam energy $\gamma_b(0)=10$, laser field $a_s(0)=0.5$, and Langmuir field $a_p(0)=0$. The initial relative phases are taken arbitrarily as $\phi_s=0$ and $\phi_L=0$. The number of sampled electrons is 300, and their initial distribution in the ponderomotive potential is uniform. Since $\mu=1.4\times10^{-3}\ll1$, $k_L\approx k_w$, the Langmuir mode has $\omega_L=\omega_p$, and $\lambda_L\approx\lambda_w$. The plasma frequency is $\omega_p=1.9\times10^{11}$ rad/s, which corresponds to a 30 GHz microwave source. We have included the effect of the laser field in the background plasma energy so that $\gamma=(1+a_s^2/2)^{1/2}$ according to $\varepsilon^2=(mc^2)^2+(pc)^2$, $p=\gamma mv$, and $\varepsilon=\gamma mc^2$. For the plasma density chosen above and hence the microwave frequency used, the phase velocity of the Langmuir mode, with the chosen wiggler period, happens to be in the vicinity of the speed of light. The choice of plasma density is directly related to the availability of microwave source.

We note that, by fixing the plasma density, electron temperature, and wiggler period, the operating parameters of the device are uniquely defined. However, the laser frequency is given externally, and to produce a plasma of exactly that density is impossible, and some frequency mismatch is, therefore, unavoidable. If the plasma density is higher than what it should be, the laser field will be reflected on the plasma-vacuum interface. We, thus, consider only negative frequency mismatch corresponding to density below the expected value. Deviations of plasma temperature make the two frequency mismatches unequal. Near the cutoff, we have $\lambda_s/\lambda_L=720$. Consequently, we fix our normalized wiggler length $Z(L)=L/\lambda_L=300$ to assure a spatially uniform laser field.

Due to the small group velocity, the laser characteristic moves along slowly. In order to integrate these equations correctly, we need to take very small step sizes. In our case, we have divided each wiggler period in 4×10^4 steps. This is exclusively a feature of our system that operates near the cutoff with a slow group velocity. The phase ψ_L in Eq. (17) along the laser characteristic is $\psi_L=-k_Lz/\mu$. The interval of Δz within which ψ_L varies by 2π is $\Delta z=\mu\lambda_L=\mu\lambda_w$, which is much less than the wiggler period. Consequently, we need a large number of grid points over one wiggler period to accurately follow ψ_L in Eq. (17).

VI. FREQUENCY MISMATCHES

We consider the generation of the Langmuir mode by examining, first, the experimentally unrealistic case of zero mismatches. In this case, the Langmuir mode grows to amplitudes much larger than unity. This solution can be understood by using the fact that ψ_L varies rapidly to take a spatial average of Eq. (17), which gives $\phi_s=0$. Consequently, $\phi_L=\Delta\phi$, and Eq. (15) becomes an equation for $\Delta\phi$. Since $\Delta\phi=0$ initially, it remains zero thereafter. With the invariance of $\Delta\phi$, Eq. (14) gives a linear growth of a_p. Without using the spatial average of Eq. (17), and solving Eqs. (14)–(17) numerically, the Langmuir amplitude is still large although it is no longer linear along the wiggler. Since the frequency doubling quadratic terms in the fluid equations are not considered here, the saturation level of the space charge field is unrealistically high, which is incompatible with our linear parametric analysis. In practice, the quadratic terms would limit the space charge field at a much lower level where the driving energy begins to leak to other frequencies. For two mismatches identically equal, similar solutions are obtained. This is because, by taking the difference between Eqs. (15) and (17), the mismatch can be eliminated to yield the same equation of $\Delta\phi$.

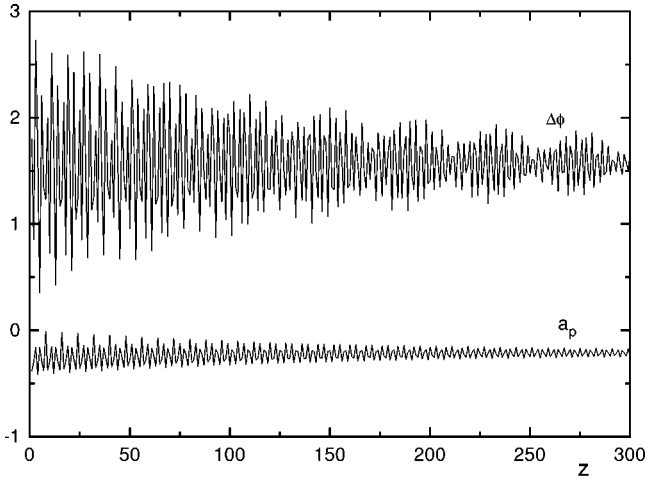

FIG. 1. The Langmuir mode a_p, and the phase $\Delta\phi$ are plotted against the normalized wiggler distance $Z=z/\lambda_L$ with $B_w=200$ G, $\Delta\omega_s^2/(ck_L)^2=-10^{-2}$, and $\Delta\omega_L^2/(ck_L)^2=-2\times10^{-2}$.

We now consider unequal mismatches. We note that the generation of the Langmuir mode depends on the ponderomotive product $a_w a_s$ only, which allows us to combine either a moderate wiggler field with a weak microwave, or a weak wiggler field with a moderate microwave source. With wiggler field $B_w=200$ G, the evolution of the Langmuir mode a_p, and the phase $\Delta\phi=(\phi_L-\phi_s)$ as a function of the normalized wiggler distance $Z=z/\lambda_L$ are shown in Fig. 1. The evolution of the phase $\Delta\phi$ according to Eqs. (15) and (17) and the cosine factor in Eq. (14) make the Langmuir mode saturate at $a_p=0.25$ with $\Delta\phi=\pi/2$. Our spatial solution along the characteristic corresponds to the temporal solution at any fixed location along the wiggler. Consequently, a uniform Langmuir mode is established in the wiggler. Here, the Langmuir mode settles down to a negative amplitude, which corresponds to a phase shift of π. Should $\psi_s=\pi$ be chosen initially, a_p would be positive. The results of Fig. 1 demonstrate the importance of the relative phases and frequency mismatches in our model. The primary message here is that the Langmuir mode with a specific wave vector can be readily driven in this system with simple equipment and weak wiggler field. A spatially uniform Langmuir mode is now established whose amplitude is limited by real conditions.

To consider beam acceleration, we then fire intermittent

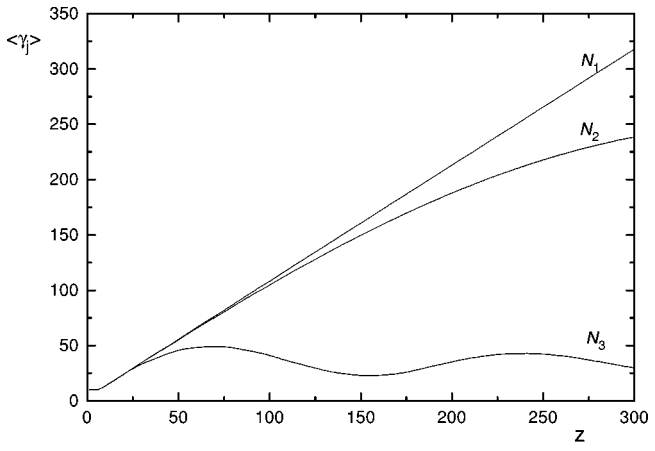

FIG. 2. The beam energy γ is plotted against the normalized wiggler distance $Z=z/\lambda_L$ with $B_w=200$ G, $N_{1,2,3}=1.188$, $1.190, 1.200\times10^{13}$ cm^3, $\Delta\phi=\pi/2$.

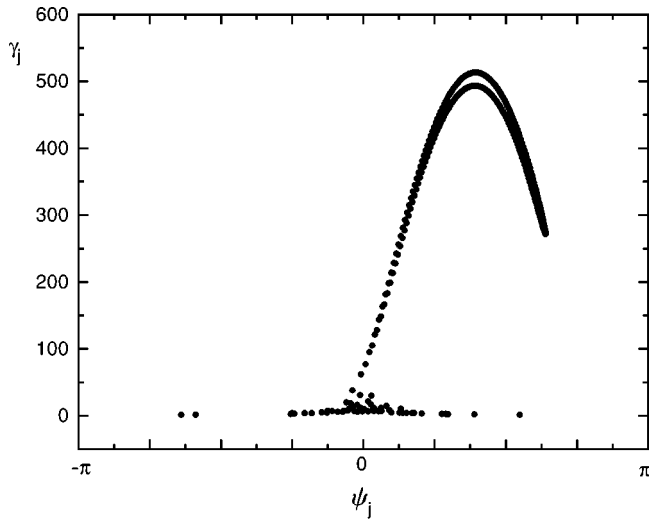

FIG. 3. Energy distribution γ_j of the sampled electrons as a function of the ponderomotive phase ψ_j in the potential well at $Z=300$ with $N=1.188\times10^{13}$ cm^3.

short electron bunches into the device. The interval between bunches corresponds to the loading time of the wiggler plasma. We then integrate Eqs. (18) and (19) along the beam characteristic in the presence of an established uniform Langmuir mode and the profiles of $\Delta\phi$ and ϕ_L. From Fig. 1, we take $\Delta\phi=\pi/2$ as input plus $\phi_L=0$. The acceleration of each beam electron depends on the phase ψ_j in the ponderomotive potential. Its evolution is a function of the velocity mismatch between the electron and the Langmuir phase velocity as described in Eq. (19). Here, the equations are integrated along the fast beam characteristic so that 100 grid points in each wiggler period are sufficient. Since the Langmuir phase velocity is a function of plasma density, we analyze the beam acceleration for several densities, all in the vicinity of $\beta_L=1$. Taking a positive amplitude with $a_p=0.25$, the results in Fig. 2 show a linear acceleration to $\gamma=320$ when $\beta_L=1$ exactly. For very small deviations with β_L slightly above unity, the beam energy in Fig. 2 shows oscillations at low levels, and likewise for deviations slightly below unity. Consequently, this puts a strong demand on monitoring the plasma density at the exact desired value, which would also control the frequency mismatch. The energy distribution of the sampled electrons in the ponderomotive well at $Z=300$ with $\beta_L=1$ is shown in Fig. 3, which shows a sizable energy distribution ranging from unity to 510.

To understand the linear growth, we examine Eqs. (18) and (19) for the case of $\beta_L=1$. We observe that Eq. (19) indicates that ψ_j approaches a constant asymptotically as β_{zj} goes to unity. For the electron energy, Eq. (18), without the small $a_s a_w$ terms, shows that $d\gamma_j/dz_b$ approaches a constant as well. The individual electron energy and, hence, the average beam energy grow linearly along the wiggler. Under these conditions, Eq. (18) becomes

$$\gamma(z_b)=\frac{\omega_p^2}{(ck_L)^2}(k_L z_b)a_p=\beta_L^2(k_L z_b)a_p. \tag{20}$$

According to Eq. (20) of linear growth, and with $a_p=0.25$, we have $\gamma=2\pi\times300a_p=460$ at the end of the wiggler, which accounts of the numerical result. Should β_L be different from unity, then neither ψ_j nor $d\gamma_j/dz_b$ is stationary as β_{zj} approaches unity, which lowers the energy gain. To summarize our findings, it is absolutely essential to choose the primary system parameters, $\omega_p, \omega_s, \mu, k_w$, such that β_L is as close to unity as possible with minimum frequency mismatch to acertain the excitation of the Langmuir mode and the acceleration of the beam over the entire wiggler. Unfortunately, Eq. (20) also claims that we are unable to increment more than 460 on the beam energy limited by the wiggler size for uniform a_s. This limitation cannot be contoured by increasing the plasma density with compatible microwave source since $\beta_L=1$ is required at any density with matching source. As density goes up, wiggler period has to go down to keep the Langmuir mode phase velocity close to the speed of light. Should we operate the system at much higher densities without shortening the wiggler period correspondingly to achieve much higher energies since β_L would be much larger than unity, we would be disappointed. The factor β_L^2 alone in Eq. (20) would not lead to higher energies since the cosine factor in Eq. (18) would set in immediately at large β_L to saturate the beam energy at low levels. Numerical integration, in this case, would require very dense grid points to accurately follow the ψ_j in the cosine factor.

VII. DISCUSSIONS AND CONCLUSIONS

For an electron beam to reach, for example, $\gamma=200$ or 100 MeV at the end of the wiggler, there is 1.6×10^{-11} J for each electron. With a beam density of 10^{10}/cm^3, this amounts to a beam energy density of $U_b=0.16$ J/cm^3. In steady state, the microwave energy density in free space U_0 and inside the plasma U_p satisfy the Poynting vector, or energy density flux, continuity across the plasma-vacuum interface with

$$U_0 c=U_p v_{gs}=U_p c^2\frac{k_s}{\omega_s}, \tag{21}$$

where v_{gs} is the group velocity in plasma. By using $\lambda_s=720\lambda_L$, we get $v_{gs}=4.2\times10^6$ cm/s. With this group velocity, it takes 70 μs to fill up the wiggler of 3 m in length

with microwave field. We can, therefore, build up a high energy density field in the plasma with a low energy density source in free space. This spatially uniform microwave field energy is then transferred to the beam of length $L_b \ll L$, which takes about 10 ns to traverse the wiggler, launched at the moment when the wiggler is completely loaded with microwave. We then have $U_b = U_p = U_0 c/v_{gs}$. Let us consider that the beam, the plasma, and the microwave have equal cross sections A. The microwave energy is then estimated by $W = U_p LA = U_b LA$. With $A = 1$ cm^2, we need a microwave energy of $W = 50$ J. With the loading time of 70 μs, the source in free space has to have a power of $P = 700$ kW. Since the group velocity is much less than the beam velocity, the wave energy could be depleted by the leading edge of a long beam. Our configuration is, therefore, suitable only to accelerate short beam bunches with, for example, $L_b = L/10$. Between one bunch and the other, the plasma has to be reloaded with microwave field. In our calculations, we have used $a_s(0) = 0.5$ in the plasma. This normalized amplitude is equivalent to a microwave energy in the plasma loaded wiggler volume $W = 40$ J. Since we are operating in pulsed mode, there is no strong power demand on the microwave source. By extending the beam intermittent time, the wiggler plasma can be loaded over a longer period with a less powerful source.

We have examined the use of a plasma loaded free-electron-laser device to accelerate an electron beam. The four entity (S,W,L,B) interaction is executed through two parametric interactions, the Raman (SWL) and the free electron laser (SWB), respectively. Our model has included the relative phases ϕ_s and ϕ_L in the fast oscillating harmonic phases $(k_s z - \omega_s t)$ and $(k_L z - \omega_L t)$. This happens to be a very important element in the dynamics of a plasma-loaded free electron device. Operating in the pulsed mode near the cutoff, the merit of a plasma-loaded free-electron device is that it can readily generate a Langmuir mode by Raman interaction with only a small wiggler field and an available microwave source in contrast to wake field and beat wave schemes. The electron beam is then efficiently accelerated by the space charge field of the Langmuir mode. Although the ponderomotive term $a_s a_w$ in the beam energy equation is negligible, the free-electron-laser interaction makes its presence through the ponderomotive phase, described by Eq. (19), due to the $\cos(\psi_j + \phi_L)$ factor in Eq. (18). Without the plasma loading, a conventional inverse free-electron-laser device would require a much larger wiggler field and microwave power to achieve the equivalent acceleration.

ACKNOWLEDGMENTS

This work was partially supported by the Conselho Nacional de Desenvolvimentos Cientifico e Tecnologico (CNPq, The Brazilian Council of Scientific and Technologic Developments).

[1] K. H. Tsui, Sol. Phys. **168**, 171 (1996).
[2] E. D. Courant, C. Pellegrini, and W. Zakowicz, Phys. Rev. A **32**, 2813 (1985).
[3] T. Tajima and J. M. Dawson, Phys. Rev. Lett. **43**, 267 (1979).
[4] M. N. Rosenbluth and C. S. Liu, Phys. Rev. Lett. **29**, 701 (1972).
[5] T. Katsouleas and J. M. Dawson, Phys. Rev. Lett. **51**, 392 (1983).
[6] P. Sprangle, E. Esarey, and A. Ting, Phys. Rev. Lett. **64**, 2011 (1990).
[7] C. E. Clayton, K. A. Marsh, A. Dyson, M. Everett, A. Lal, W. P. Leemans, R. Willians, and C. Joshi, Phys. Rev. Lett. **70**, 37 (1993).
[8] F. Amiranoff, D. Bernard, B. Cros, F. Jacquet, G. Matthieussent, P. Mine, P. Mora, J. Morillo, F. Moulin, A. E. Specka, and C. Stenz, Phys. Rev. Lett. **74**, 5220 (1995).
[9] J. L. Bobin, Opt. Commun. **55**, 413 (1985).
[10] A. Loeb and S. Eliezer, Phys. Rev. Lett. **56**, 2252 (1986).
[11] A. Serbeto and M. V. Alves, IEEE Trans. Plasma Sci. **21**, 243 (1993).
[12] C. Maroli, V. Petrillo, and R. Bonifacio, Phys. Rev. Lett. **76**, 3578 (1996).
[13] V. Petrillo and C. Maroli, Phys. Plasmas **3**, 1773 (1996).
[14] K. H. Tsui and A. Serbeto, Phys. Plasmas **4**, 2768 (1997).
[15] K. H. Tsui, Phys. Fluids B **5**, 3808 (1993).
[16] R. Courant and D. Hilbert, *Methods of Mathematical Physics* (Interscience, New York, 1962), Vol. II, Chap. II.